Analytica Chimica Acta 638 (2009) 23–28

Contents lists available at ScienceDirect

Analytica Chimica Acta

journal homepage: www.elsevier.com/locate/aca

Mesoporous silica-based electrochemical sensor for sensitive determination of environmental hormone bisphenol A

Fengran Wang, Jinquan Yang, Kangbing Wu*

Department of Chemistry, Huazhong University of Science and Technology, Wuhan 430074, PR China

ARTICLE INFO

Article history:
Received 1 December 2008
Accepted 7 February 2009
Available online 14 February 2009

Keywords:
Electrochemical sensor
Bisphenol A (BPA)
Determination
Mesoporous silica
Modified electrode

ABSTRACT

Bisphenol A (BPA) is an emerging contaminant with severe toxic effects such as disrupting endocrine system or causing cancer, therefore, developing sensitive and selective sensor for BPA is very important and interesting. Herein, MCM-41, a kind of mesoporous silica, was synthesized and then used to prepare an electrochemical sensor for BPA. For better comparison, carbon nanotubes, activated carbon, silica gel and graphite were also employed to prepare electrochemical sensor for BPA. The electrochemical behaviors of BPA at different electrochemical sensors were investigated. Compared with other sensors, the MCM-41 sensor greatly enhances the response signal of BPA due to the large active surface area and high accumulation efficiency. The effects of pH value, accumulation time and sensor composition were examined. The linear range is from 2.2×10^{-7} to 8.8×10^{-6} mol L^{-1}, and the limit of detection is evaluated to be 3.8×10^{-8} mol L^{-1}. Finally, the MCM-41 sensor was successfully employed to determine BPA in water samples.

© 2009 Elsevier B.V. All rights reserved.

1. Introduction

Bisphenol A (2,2-bis (4-hydroxyphenyl) propane, BPA) is an organic compound that widely used in the plastic industry as a monomer for producing epoxy resins and polycarbonate. In our life, BPA is ubiquitous since it can be released into the environment from bottles, packaging, landfill leachates as well as plastics plants [1–5]. BPA was non-biodegradable and highly resistant to chemical degradation, so that the concentration of BPA in the environmental is frequently high [6,7]. A large number of researches have shown that BPA can mimic and interfere with hormonal activities by disrupting growth, development and reproduction [8–12], thus, BPA has been identified as an important endocrine disrupting compound (EDC). Most importantly, BPA was found to possibly cause cancer, and an association between BPA and breast cancer has been discovered [13,14]. Therefore, it is very important and interesting to establish sensitive method for the determination of BPA.

Various methods such as high-performance liquid chromatography (HPLC) [15,16], liquid chromatography–mass spectrometry (LC–MS) [17,18], gas chromatography–mass spectrometry (GC–MS) [19–21] and fluorimetry [22,23], have been reported for the determination of BPA. Otherwise, BPA can be oxidized and exhibits electrochemical activity since it contains phenolic hydroxy groups. Consequently, electrochemical removal of BPA based on its oxidation was successfully fulfilled [24,25], and HPLC coupled electrochemical detection was also reported for the determination of BPA [26–28].

Electrochemical sensors have great potential for environmental monitoring because of their portability, field-deployability, excellent sensitivity (in low ppb levels), automation, short analysis time, low power consumption and inexpensive equipment. Although BPA is electrochemical active, direct determination of BPA using electrochemical sensor is rare because the response of BPA at traditional electrochemical sensor is very poor. To overcome these drawbacks, novel sensing material with high sensitivity and rapid response must be developed.

Since the discovery of ordered mesoporous silica molecular sieves [29], the interest in this research field has expanded all over the world. With the characteristics such as highly uniform channels, large surface area, narrow pore-size distribution, tunable pore sizes over a wide range, and so on, mesoporous materials have attracted considerable attention, and obtained wide applications in catalysis as well as in other realms of chemistry. Undoubtedly, these excellent properties will result in better charge transport and improved electrochemical signal, so mesoporous material is considered as a promising sensing material for electrochemical sensor. For instance, the mesoporous silica was successfully used to improve the electrochemical responses of heavy metal ions [30], nitroaromatic compounds [31] as well as biomolecules [32].

Herein, a kind of mesoporous silica molecular sieves: MCM-41 was synthesized according to the published method using cationic surfactant as the structure-directing template. After that, the

* Corresponding author. Tel.: +86 27 8754 3632; fax: +86 27 8754 3632.
E-mail address: kbwu@mail.hust.edu.cn (K. Wu).

0003-2670/$ – see front matter © 2009 Elsevier B.V. All rights reserved.
doi:10.1016/j.aca.2009.02.013

resulting MCM-41 was mechanically mixed with graphite powder and paraffin oil, resulting in a MCM-41 electrochemical sensor. Otherwise, multi-wall carbon nanotube (MWNT), activated carbon, silica gel and graphite were also used to prepare electrochemical sensor for BPA according to the similar method. The electrochemical responses of BPA at different sensors were compared. It was found that the response signal of BPA remarkably improved at MCM-41 sensor, suggesting that MCM-41 is an excellent sensing material for BPA. The parameters such as pH value, accumulation time and sensor composition were optimized. Finally, a sensitive and convenient electrochemical method was proposed for the determination of BPA based on the MCM-41 sensor, which used to detect BPA in water samples.

2. Experimental

2.1. Reagent

Bisphenol A (BPA, 97%) was purchased from Acros (New Jersey, USA). Cetyltrimethylammonium bromide (CTAB, purity >99.0%), tetraethyl orthosicate (TEOS, analytical grade, SiO_2 purity >28.4%), graphite powder (spectral reagent), paraffin oil (analytical grade), silica gel (200–300 mesh) and activated carbon were purchased from the Siompharm Group Chemical Reagent Co. Ltd., China. MWNT (purity >98%) was obtained from Shenzhen Nanotech Port Co. Ltd., China. All the chemicals were used directly without further purification.

2.2. Instruments

Electrochemical measurements were carried out using 610B electrochemical analyzer (Shanghai Chenhua Co., China) in a conventional three-electrode system. The working electrode is MCM-41 sensor, the reference electrode is a saturated calomel electrode, and the auxiliary electrode is a platinum wire.

Scanning electron microscopy (SEM) was performed with a FEI-Quanta 200 microscope.

2.3. Synthesis of MCM-41

MCM-41 was synthesized as the reported method [33] using CTAB as the template. A solution of CTAB in NaOH was prepared and stirred at 298 K. After that, the silica source (TEOS) was added into the solution under stirring to give a gel mixture with following molar compositions: 1 SiO_2/0.25 NaOH/0.1 CTAB/100 H_2O. After 30 min of stirring at 298 K, the mixture was sealed and then heated at 343 K for 24 h under static conditions. The resulting solid precipitate was recovered by filtration, washed with deionized water and then dried at 80 °C overnight. Finally, the dried solid precipitate was calcined at 823 K for 6 h to remove CTAB and form mesopores. The morphology and the grain size of calcined MCM-41 were characterized using SEM, which is shown in Fig. 1. From the SEM image, it is very clear that the synthesized MCM-41 is composed of well-dispersed spherical nanoparticles.

2.4. Preparation of MCM-41 electrochemical sensor

Firstly, the synthesized MCM-41 (0.15 g) was mechanically mixed with graphite powder (0.85 g) and paraffin oil (0.4 mL) in a carnelian mortar to give a homogenous MCM-41 modified carbon paste. Secondly, the resulting carbon paste was tightly pressed into the end cavity (3 mm in diameter) of sensor body, and the surface was polished on a smooth paper. The pure graphite sensor was prepared by the same procedure but without MCM-41. Otherwise, the MWNT sensor, silica gel sensor and activated carbon sensor were fabricated according to the same procedure.

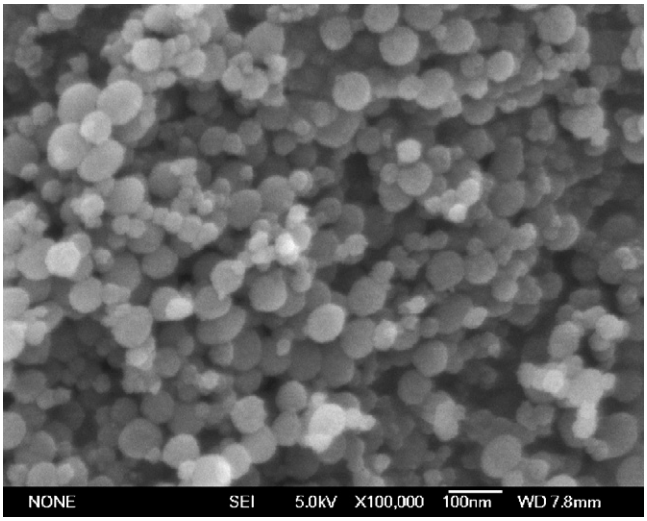

Fig. 1. SEM image of MCM-41.

2.5. Analytical procedure

Unless otherwise stated, pH 8.0 phosphate buffer (0.1 mol L^{-1}) was used as the determining medium for BPA. After 3-min accumulation, the differential pulse voltammetry images from 0.10 to 0.70 V were recorded, and the oxidation peak current was measured for BPA.

3. Results and discussion

3.1. Electrochemical properties of MCM-41 sensor

The electrochemical responses of $K_3[Fe(CN)_6]$ at different sensors were studied using cyclic voltammetry (CV) to illustrate the electrochemical properties of MCM-41 sensor. Fig. 2 depicts the CV images of $K_3[Fe(CN)_6]$ under different scan rates at graphite sensor (A), activated carbon sensor (B), MWNT sensor (C), silica gel sensor (D) and MCM-41 sensor (E). During the cyclic sweep from 0.60 to −0.20 V, a pair of redox peaks is observed at all sensors. As gradually increasing the scan rate (ν) from 50 to 200 mV s^{-1}, the reduction peak current (i_{pc}) and oxidation peak current (i_{pa}) increase linearly with the square root of scan rate, shown in the insert plot. The linear relationship between i_p and $\nu^{1/2}$ indicates that the electrochemical process of $K_3[Fe(CN)_6]$ is controlled by diffusion.

At the graphite sensor (Fig. 2a), the reduction peak and the corresponding oxidation peak separate largely. The peak potential separation ($\Delta E_p = E_{pa} - E_{pc}$) is as large as 300 mV, suggesting that the reversibility of $K_3[Fe(CN)_6]$ is poor at the graphite sensor. However, the E_{pc} shifts positively and the E_{pa} shifts negatively at other sensors, obviously lowering the ΔE_p. For example, the values of ΔE_p at activated carbon sensor, MWNT sensor, silica gel sensor and MCM-41 sensor are 200, 110, 90 and 80 mV. Therefore, the electrode process of $K_3[Fe(CN)_6]$ becomes more reversible at these sensors. According to Nicholson's theory, the standard heterogeneous rate constant (k^o) gradually increases with decreasing the value of ΔE_p. Therefore, the MCM-41 sensor facilitates the electron transfer of $K_3[Fe(CN)_6]$. Otherwise, the peak currents of $K_3[Fe(CN)_6]$ slightly increase at the activated carbon sensor, MWNT sensor and silica gel sensor, compared with those at the graphite sensor. However, the peak currents remarkably increase at the MCM-41 sensor in contrast to those at other sensors. According to Randles–Sevčik

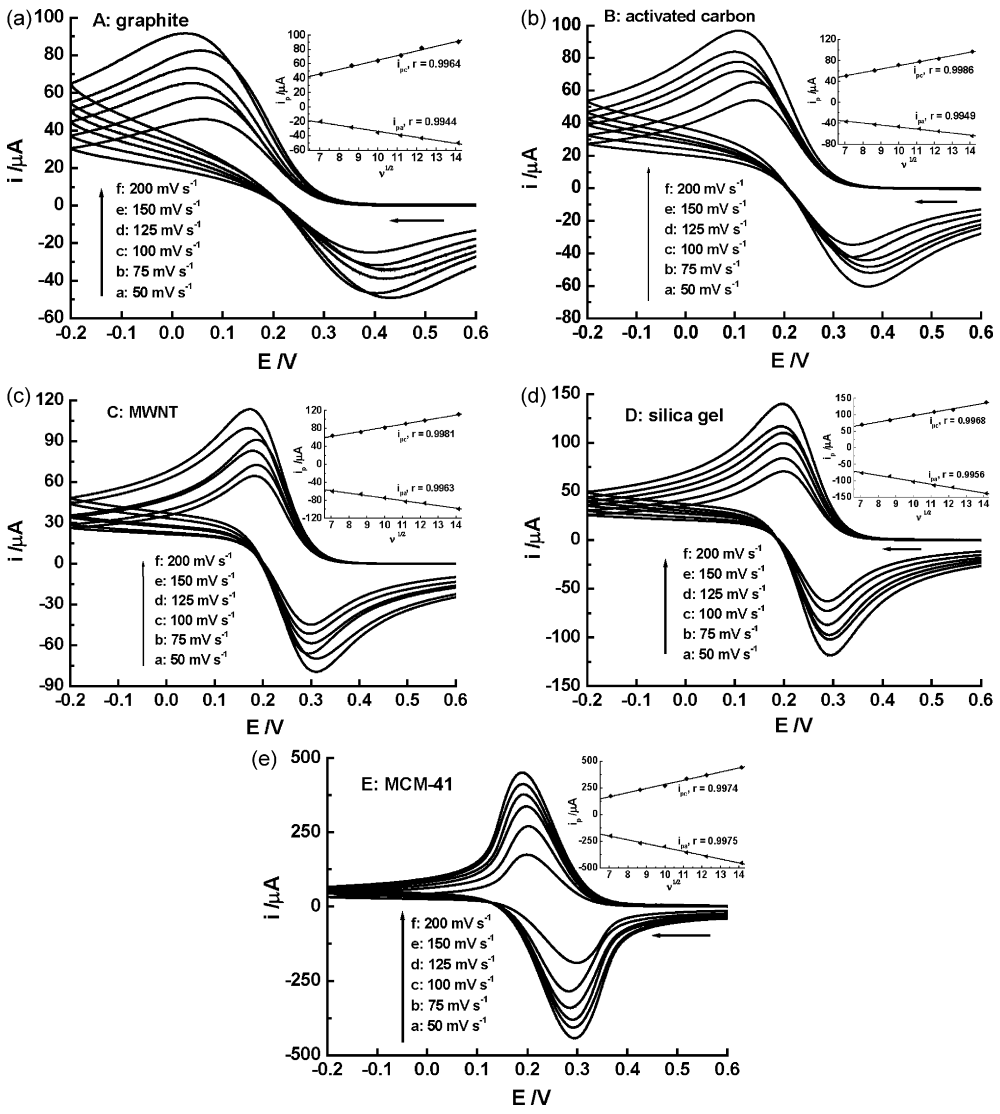

Fig. 2. CV images of $K_3[Fe(CN)_6]$ under different scan rates at graphite sensor (a), activated carbon sensor (b), MWNT sensor (c), silica gel sensor (d) and MCM-41 sensor (e). Insert plot: i_p versus $\nu^{1/2}$.

equation, the higher peak current means larger electrode area. Undoubtedly, the MCM-41 greatly improves the active area of sensor surface, compared with silica gel, MWNT, activated carbon and graphite. In brief, conclusion can be made from Fig. 2, that the MCM-41 sensor exhibits more excellent properties, maybe attributed to the specific and uniform mesopores.

3.2. Electrochemical response of BPA

In pH 8.0 phosphate buffer, the electrochemical responses of BPA at different electrochemical sensors were investigated using CV, which is shown in Fig. 3. At the graphite sensor (curve a), only an oxidation peak is observed at 0.43 V during the successive cyclic sweeps from 0.10 to 0.70 V. The peak height is low, suggesting that the response of BPA at graphite sensor is poor. In addition, the electrochemical responses of BPA at activated carbon sensor (curve b), MWNT sensor (curve c), silica gel sensor (curve d) and MCM-41 sensor (curve e) were individually examined. Within the potential window from 0.10 to 0.70 V, only an oxidation peak is also observed at these sensors, indicating that the oxidation of BPA is totally reversible. Compared with those at the graphite sensor, the oxidation signals of BPA do not increase at activated carbon sensor, MWNT sensor and silica gel sensor. However, the oxidation signals

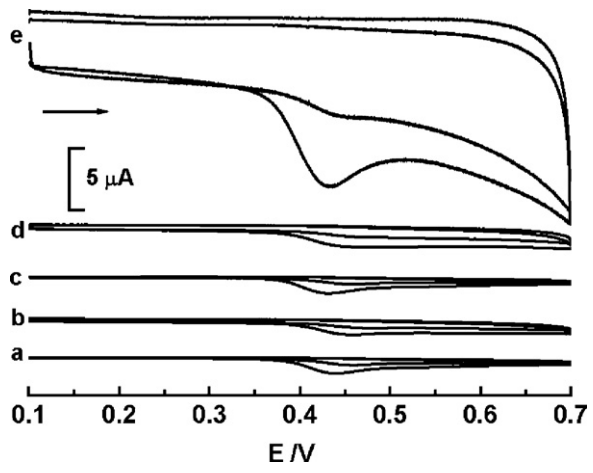

Fig. 3. Successive cyclic voltammograms of 1.0×10^{-5} mol L^{-1} BPA in pH 8.0 phosphate at graphite sensor (curve a), activated carbon sensor (curve b), MWNT sensor (curve c), silica gel sensor (curve d) and MCM-41 sensor (curve e). Scan rate: 100 mV s^{-1}.

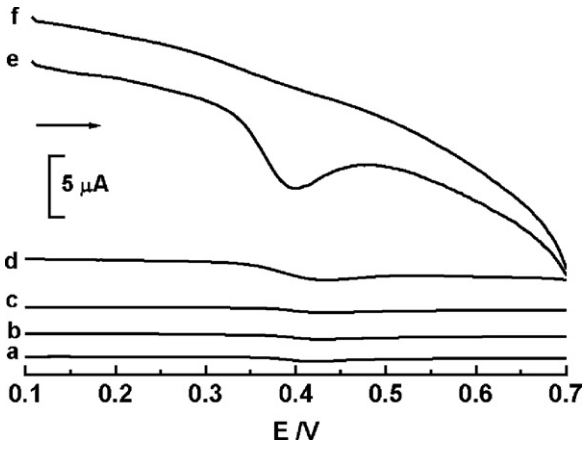

Fig. 4. DPV images of 2.5×10^{-6} mol L^{-1} BPA at graphite sensor (curve a), activated carbon sensor (curve b), MWNT sensor (curve c), silica gel sensor (curve d) and MCM-41 sensor (curve e). Curve (f): DPV images of MCM-41 sensor without BPA. Accumulation time: 3.0 min.

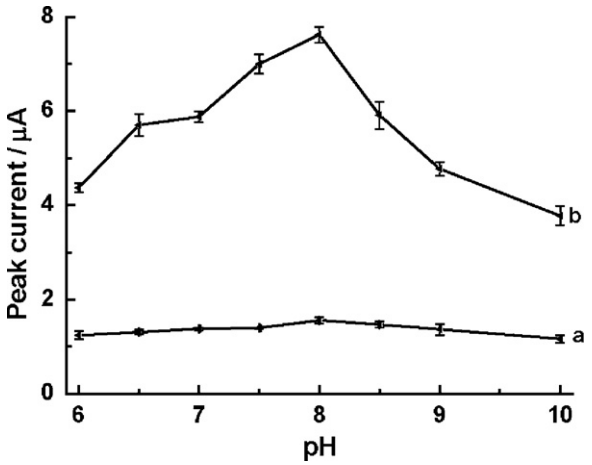

Fig. 5. Effect of pH value on the peak current of 1.0×10^{-5} mol L^{-1} BPA at graphite sensor (curve a) and MCM-41 sensor (curve b).

of BPA remarkably increase at the MCM-41 sensor. So the MCM-41 is more active towards BPA and can significantly improve the sensitivity of determining BPA, compared with silica gel, MWNT, activated carbon and graphite. In addition, it is very clear from Fig. 3, that the oxidation peak currents of BPA obviously decline during the second anodic sweep. This may be caused by the fact that the oxidative product of BPA adsorbs at sensor surface. Therefore, the oxidation signal during the first anodic sweep was recorded for BPA in the following studied.

The chronocoulometry curves of different sensors in the absence and presence of BPA were recorded to infer the adsorption of BPA at sensor surface. According to Anson's theory, the plot of charge (Q) versus $t^{1/2}$ is a straight line, and the charge corresponding to adsorbed component (Q_{ads}) can be easily achieved from the intercept difference. After the addition of BPA, the intercepts of Q–$t^{1/2}$ plot slightly increase at graphite sensor, activated carbon sensor, MWNT sensor and silica gel sensor, suggesting that the adsorption of BPA at these sensors is very weak. However, the intercept at MCM-41 sensor increases two times after adding BPA, revealing that MCM-41 offers highly efficient accumulation towards BPA. There is no doubt that the MCM-41 sensor obviously enhances the oxidation signals to BPA.

The electrochemical responses of low concentration of BPA at different sensors were further studied using differential pulse voltammetry (DPV) since DPV possesses high sensitivity and excellent resolution. Fig. 4 depicts the DPV images of 2.5×10^{-6} mol L^{-1} BPA at graphite sensor (curve a), activated carbon sensor (curve b), MWNT sensor (curve c), silica gel sensor (curve d) and MCM-41 sensor (curve e). Otherwise, the DPV images of MCM-41 sensor in determining medium without BPA were also given in curve (f) for better understanding. As expected, a well-shaped oxidation peak appears at the MCM-41 sensor, and the oxidation peak currents significantly improved, compared with those at other sensors. As testified above, the MCM-41 sensor exhibits larger active surface area and highly efficient accumulation to BPA. Therefore, the electrochemical oxidation of BPA at MCM-41 sensor becomes more easily and the oxidation signals remarkably improved.

3.3. Optimization of detection at MCM-41 sensor

The electrochemical responses of BPA were studied in different mediums such as pH 6.0, 6.5, 7.0, 7.5, 8.0 phosphate buffer, pH 8.5, 9.0 and 10.0 tris–HCl buffer. Fig. 5 shows the effect of pH value on the oxidation peak current of BPA at graphite sensor (curve a) and MCM-41 sensor (curve b). When the pH value gradually increases from 6.0 to 8.0, the oxidation signal of BPA also gradually improves at graphite sensor and MCM-41 sensor. In addition, the oxidation peak potential of BPA shifts negatively with increasing pH value, revealing that proton takes part in the oxidation of BPA. When pH value improves, the electrochemical oxidation of BPA becomes easy, so the peak current gradually increases. However, the oxidation signal of BPA gradually decreases as furthering increasing pH value from 8.0 to 10.0, maybe caused by the fact that the activity of sensor lowers at higher pH value. Undoubtedly, determination of BPA at pH 8.0 has the highest sensitivity. Moreover, the background current is relatively low and the oxidation peak is well shaped at pH 8.0. Therefore, the pH 8.0 phosphate buffer was used as the determining medium for BPA. From Fig. 5, it is also apparent that the oxidation signal of BPA greatly increased at the MCM-41 sensor, which explained as above.

Fig. 6 depicts the influence of content of MCM-41 on the oxidation peak current of BPA. As gradually improving the content of MCM-41 from 0% to 15%, the peak current of BPA greatly enhances. When further increasing the content from 15% to 20%, the oxidation peak current of BPA increases slightly, and the plot becomes curved. With increasing the content of MCM-41, the effective surface area and the accumulation efficiency also improve. Consequently, the surface concentration of BPA increases and then the oxidation peak current also enhances. However, the oxidation peak current of BPA dramatically decreases when the content of MCM-41 increases from 20% to 25%, suggesting that too much MCM-41 is unbeneficial for BPA sensing. Although MCM-41 possesses promising properties, its

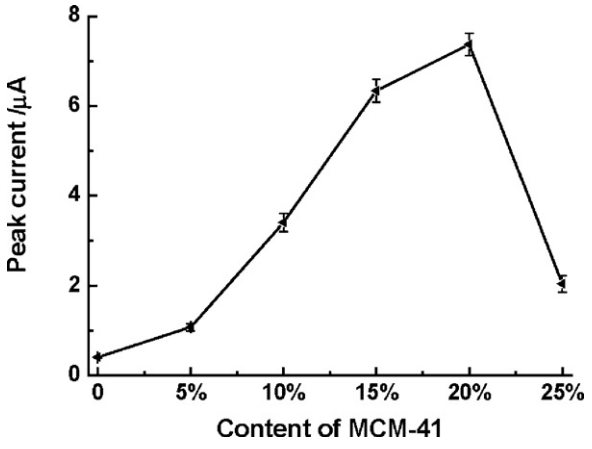

Fig. 6. Effect of content of MCM-41 on the peak current of 2.5×10^{-6} mol L^{-1} BPA.

Table 1
Determination of BPA in lake water samples.

Water sample	Spiked (mol L^{-1})	Expected (mol L^{-1})	Found (mol L^{-1})	R.S.D. (n = 5)	Recovery
Yujia Lake	0.00		4.13×10^{-7}		
	5.00×10^{-7}	9.13×10^{-7}	8.95×10^{-7}	3.5%	96.4%
Zuiwanting Lake	0.00		8.36×10^{-7}		
	1.00×10^{-6}	1.836×10^{-6}	1.794×10^{-6}	3.6%	95.8%
Nanmen Lake A	0.00		0.00		
	2.00×10^{-6}	2.00×10^{-6}	1.89×10^{-6}	2.6%	94.5%
Nanmen Lake B	0.00		0.00		
	8.00×10^{-7}	8.00×10^{-7}	7.79×10^{-7}	6.4%	97.4%
Eastern Lake A	0.00		0.00		
	5.00×10^{-7}	5.00×10^{-7}	5.36×10^{-7}	3.8%	107.2%
Eastern Lake A	0.00		0.00		
	3.00×10^{-6}	3.00×10^{-6}	2.74×10^{-6}	3.2%	91.3%

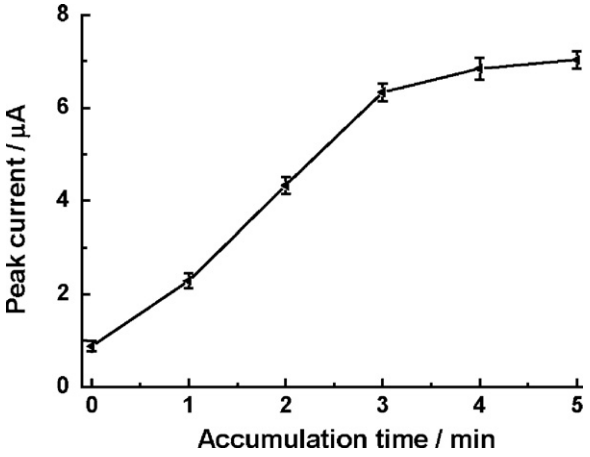

Fig. 7. Influence of accumulation time on the peak current of 2.5×10^{-6} mol L^{-1} BPA at MCM-41 sensor.

electric conductivity is very poor. So, the conductivity of MCM-41 sensor will gradually lower with improving the content of MCM-41, blocking the electron transfer and increasing the background current. As a result, the oxidation peak current of BPA contrarily decreases when the content of MCM-41 is higher than 20%. In this work, the best content of MCM-41 is selected as 15%.

Fig. 7 shows the influence of accumulation time on the oxidation peak current of BPA at the MCM-41 sensor. When the accumulation time increases from 0 to 3 min, the oxidation peak current of BPA linearly increases. Accumulation improves the surface amount of BPA and then enhances the oxidation signal of BPA. As further extending the accumulation time from 3 to 5 min, the oxidation peak current of BPA slightly increases, suggesting that the surface amount of BPA tends to a limiting value. So, the sensitivity of MCM-41 sensor does not improve when the accumulation time is beyond 3 min. Considering sensitivity and working efficiency, the accumulation time is controlled at 3 min when determining BPA.

3.4. Analytical performance of MCM-41 sensor

The MCM-41 sensor was used for single measurement to achieve better reproducibility. The precision between multiple MCM-41 sensors was estimated by determining the response of BPA at 10 MCM-41 sensors. The relative standard deviation (R.S.D.) is 6.4%, indicative of acceptable fabrication reproducibility and good determining precision.

To evaluate the interferences of other phenolic compounds on the determination of BPA, a systematic studies were carried out. The oxidation peak currents of 2.50×10^{-6} mol L^{-1} BPA in the absence and in the presence of different concentrations of interferents were measured, respectively. Based on this, the peak current change of BPA can be achieved. It was found that 1.25×10^{-4} mol L^{-1} o-nitrophenol, m-nitrophenol and p-nitrophenol; 2.75×10^{-5} mol L^{-1} o-aminophenol, m-aminophenol and p-aminophenol; 3.75×10^{-6} mol L^{-1} phenol; 2.50×10^{-6} mol L^{-1} 4-chlorophenol, almost have no influence on the determination of BPA when the peak current change is lower that 10%.

Under the optimized conditions, the variation of oxidation peak current with concentration was studied using DPV after 3-min accumulation. It was found that the oxidation peak current of BPA is proportional to its concentration over the range from 2.2×10^{-7} to 8.8×10^{-6} mol L^{-1}, obeying the following equation: $i_p = 0.5376 + 2.833 \times 10^6 C$ (i_p in μA, C in mol L^{-1}, correlation coefficient is 0.997). Otherwise, the sensitivity of MCM-41 sensor was also evaluated based on a three signal-to-noise ratio. After 3-min accumulation, the limit of detection is as low as 3.8×10^{-8} mol L^{-1}. It is necessary to state that the sensitivity will be further improved with increasing the accumulation time.

3.5. Determination of BPA in water samples

To demonstrate its suitability and potential for sample analysis, the proposed MCM-41 sensor was used to determine BPA in different lake water samples. The water samples were collected from the Yujia Lake, the Zuiwanting Lake and the Nanmen Lake in Huazhong University of Science and Technology, as well as from the Eastern Lake in Wuhan City. The collected water samples were filtered through a 0.45 μm filter membrane before analysis. After that, 5.00 mL water sample was added into 5.00 mL pH 8.0 phosphate buffer, and then analyzed according to Section 2.5. Each sample solution undergoes five parallel detections, and the R.S.D. is below 6.5%, suggesting that the results obtained by MCM-41 sensor are acceptable. The concentration of BPA in water sample was obtained by the standard addition method, which is shown in Table 1. In the water samples of Yujia Lake and Zuiwanting Lake, BPA was detected. However, BPA was not detected in the water samples of Nanmen Lake and Eastern Lake. Otherwise, different concentrations of BPA standard were spiked into the water samples, and then analyzed under the same conditions. From the spiked value and the detected value, the recovery was easily obtained. The recovery of BPA standard is in the range from 91.3% to 107.2%, suggesting that the recovery of MCM-41 sensor is satisfactory and the determination of BPA using MCM-41 is feasible.

4. Conclusion

A kind of mesoporous silica molecular sieves, MCM-41, was synthesized using CTAB as the template, and then used to develop

an electrochemical sensor for BPA. Owing to the regular and specific mesoporous networks, MCM-41 sensor possesses large surface area and highly efficient accumulation ability, compared with other sensors such as carbon nanotubes, silica gel, activated sensor and graphite. Therefore, the oxidation signal of BPA at the MCM-41 sensor remarkably improved, and then a novel electrochemical method was proposed for the determination of BPA, which successfully demonstrated with water samples.

Acknowledgement

The authors are grateful for the financial support from National Basic Research Program of China (973 Program, 2009CB320300). The Center of Analysis and Testing of Huazhong University of Science and Technology is thanked for its help in the SEM observation.

References

[1] J.Y. Hu, T. Aizawa, S. Ookubo, Environ. Sci. Technol. 36 (2002) 1980.
[2] D.W. Kolpin, E.T. Furlong, M.T. Meyer, E.M. Thurman, S.D. Zaugg, L.B. Barber, H.T. Buxton, Environ. Sci. Technol. 36 (2002) 1202.
[3] B. Hileman, Chem. Eng. News 81 (2003) 7.
[4] X.L. Jin, G.B. Jiang, G.L. Huang, J.F. Liu, Q.F. Zhou, Chemosphere 56 (2004) 1113.
[5] R.A. Torres, C. Pétrier, E. Combet, F. Moulet, C. Pulgarin, Environ. Sci. Technol. 41 (2007) 297.
[6] H.B. Lee, T.E. Peart, Water Qual. Res. J. Can. 35 (2000) 283.
[7] C.A. Staples, P.B. Dorn, G.M. Klecka, S.T. O'Block, D.R. Branson, L.R. Harris, Chemosphere 40 (2000) 521.
[8] N.B. Jonathan, R. Steinmetz, Trends Endocrinol. Metab. 9 (1998) 124.
[9] S. Jobling, M. Nolan, C.R. Tyler, G. Brighty, J.P. Sumpter, Environ. Sci. Technol. 32 (1998) 2498.
[10] W.G. Foster, Water Qual. Res. J. Can. 36 (2001) 253.
[11] W. Welshons, K.A. Thayer, B.M. Judy, J.A. Taylor, E.M. Curran, F.S. vom Saal, Environ. Health Perspect. 111 (2003) 994.
[12] J.H. Kang, F. Kondo, Y. Katayama, Toxicology 226 (2006) 79.
[13] N.E. Skakkebaek, E.R. Meyts, N. Jorgensen, E. Carlsen, P.M. Petersen, A. Giwercman, APMIS 106 (1998) 3.
[14] M.T. Monica, C.M. Markey, P.R. Wadia, E.H. Luque, B.S. Rubin, C. Sonnenschein, A.M. Soto, Endocrinology 146 (2005) 4138.
[15] Y. Watabe, T. Kondo, M. Morita, N. Tanaka, J. Haginaka, K. Hosoya, J. Chromatogr. A 1032 (2004) 45.
[16] J.J. Ou, L.H. Hu, L.G. Hu, X. Li, H.F. Zou, Talanta 69 (2006) 1001.
[17] M. Liu, Y. Hashi, F. Pan, J. Yao, G. Song, J.M. Lin, J. Chromatogr. A 1133 (2006) 142.
[18] H. Sambea, K. Hoshina, K. Hosoya, J. Haginaka, J. Chromatogr. A 1134 (2006) 16.
[19] Z. Kuklenyik, J. Ekong, C.D. Cutchins, L.L. Needham, A.M. Calafat, Anal. Chem. 75 (2003) 6820.
[20] M. Kawaguchi, R. Ito, N. Endo, N. Okanouchi, N. Sakui, K. Saito, H. Nakazawa, J. Chromatogr. A 1110 (2006) 1.
[21] G. Gatidou, N.S. Thomaidis, A.S. Stasinakis, T.D. Lekkas, J. Chromatogr. A 1138 (2007) 32.
[22] X. Wang, H. Zeng, L. Zhao, J.M. Lin, Anal. Chim. Acta 556 (2006) 313.
[23] J. Fan, H. Guo, G. Liu, P. Peng, Anal. Chim. Acta 585 (2007) 134.
[24] H. Kuramitz, Y. Nakata, M. Kawasaki, S. Tanaka, Chemosphere 45 (2001) 37.
[25] H. Kuramitz, M. Matsushita, S. Tanaka, Water Res. 38 (2004) 2331.
[26] J. Sajiki, J. Chromatogr. B 755 (2001) 9.
[27] K. Ouchi, S. Watanabe, J. Chromatogr. B 780 (2002) 365.
[28] J. Sajiki, J. Chromatogr. B 783 (2003) 367.
[29] C.T. Kresge, M.E. Leonowicz, W.J. Roth, J.C. Vartuli, L.J.S. Beck, Nature 359 (1992) 710.
[30] W. Yantasee, B. Charnhattakorn, G.E. Fryxell, Y.H. Lin, C. Timchalk, R.S. Addleman, Anal. Chim. Acta 620 (2008) 55.
[31] H.X. Zhang, A.M. Cao, J.S. Hu, L.J. Wan, S.T. Lee, Anal. Chem. 78 (2006) 1967.
[32] Y.H. Zeng, J.Q. Yang, K.B. Wu, Electrochim. Acta 53 (2008) 4615.
[33] A. Galarneau, M. Cangiotti, F. Renzo, F. Fajula, M.F. Ottaviani, J. Phys. Chem. B 110 (2006) 4058.